Progress In Electromagnetics Research B, Vol. 70, 131–147, 2016

Retrieval of the Frequency-Dependent Effective Permeability and Permittivity of the Inhomogeneous Material in a Layer

Armand Wirgin*

Abstract—This study is focused on how to obtain the effective or equivalent properties of inhomogeneous materials, which, contrary to the usual metamaterials, are assumed to possess only a sandwich-like form of heterogeneity. More specifically, the aim is to see how the method of inversion, and associated type and amount of data, condition the outcome of the inversion, notably as concerns the possibility or not of exotic features such as simultaneous negative permittivity and permeability in certain frequency intervals. Two inversion schemes are considered and compared: the Nicolson-Ross-Weir (NRW) scheme and an optimization scheme. The adopted form of the optimization scheme provides only numerical retrievals, but it applies to any number of far-field data couples, which fact makes it a useful tool for determining whether the retrieved properties of an inhomogeneous material really are independent of the angle of incidence as is required for effective properties. It is shown, via the optimization scheme, that the apparently infinite number of solutions predicted by the NRW scheme is reduced to a single solution — closest to the predictions of a mixture model — when the constraint of independence with respect to angle of incidence is invoked. Moreover, this solution exhibits none of the exotic features of the properties of the usual metamaterials except temporal dispersion and loss even when the component materials of the inhomogeneous layer are neither dispersive nor lossy.

1. INTRODUCTION

Obtaining the constitutive parameters (or frequency-dependent functions) of a material encased within a layer from the observed reflection and transmission response of the latter to a plane wave is an inverse problem (IP) [1, 2], sometimes qualified [3] as a (parameter-) retrieval problem. If the material is homogeneous [1, 6, 7, 13], one expects to retrieve the true constitutive parameters by this means. If the material is inhomogeneous (e.g., a metamaterial; [3, 8, 11], one hopes to recover what is often termed the effective or equivalent constitutive parameters of the supposed-homogeneous material in the layer.

A particularly-illuminating illustration of the ill-posed nature [5] of IP's can be perceived in the exact, mathematically-explicit solutions for the permittivity and permeability of a supposed-homogeneous layer resulting from the Nicolson-Ross-Weir (NRW) technique [10, 18]: these mathematical (as opposed to numerical) retrievals for reflectivity and transmissivity data turn out to be both infinite in number, and unstable in the neighborhoods of the so-called Fabry-Pérot resonance frequencies [1, 7]. A more common way to solve IP, applicable to other specimen geometries for which the solutions cannot be obtained in exact, mathematically-explicit form, is based on optimization techniques, i.e., iterative minimization of a cost functional which is a measure of the discrepancy between the observed response and trial responses incorporating trial values of the constitutive parameters. The ill-posedness shows up in this technique by the fact that the cost functional exhibits a series of more-or-less deep minima in the multidimensional (2D in the case of real permittivity and permeability) constitutive parameter search region, and the locations of these minima may vary considerably with observed-data noise and/or

Received 9 August 2016, Accepted 30 October 2016, Scheduled 14 November 2016
* Corresponding author: Armand Wirgin (wirgin@lma.cnrs-mrs.fr).
The author is with the Aix Marseille University, CNRS, Centrale Marseille, LMA, Marseille, France.

uncertainty of the model (termed the retrieval model) employed for the generation of trial values of the sought-for parameters.

Actually, the NRW technique employs the same basic ingredients as the optimization technique since it compares observed data to trial data resulting from the employment of a retrieval model that appeals to the exact solutions of the forward problem of a plane wave impinging on a flat-faced, homogeneous layer (henceforth, each face of the layer is considered to occupy the entire x-y plane for a particular value of z). If the material in the layer is really homogeneous, then the response, takes the form, as assumed in the retrieval model, of a reflected plane wave (RPW) and a transmitted plane wave (TPW) outside the layer. If, on the other hand, the material in the layer is really inhomogeneous, then the response outside the layer is generally not reducible to a single RPW and a single TPW, i.e., homogeneous plane waves are also sent out in other directions (scattering), and, in addition, surface waves make their appearance. In this situation, which we term *model discordance*, the retrieval model is not telling the same story as the observed data since the retrieval model only accounts for one RPW and one TPW, whereas the data says that there are other waves as well. This discordance shows up in another manner when one produces the data by simulation [16] rather than by experimental observation. Suppose, for instance, that the inhomogeneity in the layer takes the form of two spheres, each enclosing a non-lossy material that is different from that of the homogeneous non-lossy host material in the layer. Then, six (real) constitutive and four geometrical parameters are necessary to simulate the response of the inhomogeneous layer to a solicitation whereas only two (real) constitutive and one geometrical parameters are employed in the homogeneous-layer retrieval model. This *parameter reduction* is, of course, the desirable feature in *homogenization* techniques which seek to characterize inhomogeneous materials by means of effective or equivalent homogenous surrogates. But, this desirable feature can be accompanied by undesirable, or at least unexpected, features in the process and results of inversion. For instance: violation of the principle of conservation of energy (when scattering is produced, since the sum of the reflected and transmitted energy is not equal to the incident energy when there is no dissipation in the layer) unless the constitutive parameters of the homogenized layer are assumed to be complex, in which case the parameter reduction is less pronounced since the number of to-be-retrieved parameters is four (i.e., two real parts and two imaginary parts). Another, perhaps unexpected feature, in the case in which the component materials in the inhomogeneous layers are all temporally non-dispersive, is that the homogenized material turns out to be temporally-dispersive and, in some cases, even anomalously-dispersive. All these features make the inverse problem, associated with the homogenization procedure, more difficult to solve, in that they have effects on the ill-posedness that are not easy to predict and understand.

A recurrent question is whether exotic features of retrieved constitutive parameters, such as negative (real and/or imaginary parts of) permittivities and permeabilities (in the electromagnetic metamaterial context: [3, 11, 16, 17]) of the homogenized materials, really exist (i.e., are physically-realistic [8, 15, 17]) or are just artifacts of the inversion procedure ([9, 20]. It is not evident how to deal with such a question because a constitutive parameter is never a direct result of measurement, but rather an indirect result, precisely that of the aforementioned inverse problem which gives rise to the abnormal (or even normal) features [15]. This dilemma is usually resolved by invoking various physical constraints such as passivity [15, 16, 20], or considering the feature to be physically-realistic if it is also the indirect result of other types of observations (and associated inverse problem solutions) [12]. But before resorting to this expedient, one should examine in detail how the the retrieved parameters depend on the various ingredients of the IP. This constitutes the principal task of the present investigation.

To achieve this, we shall invert the response of two types of layers. Both of these layers give rise to a single RPW and a single TPW under plane wave solicitation although the first type is homogeneous and the second inhomogeneous. The reason why our inhomogeneous layer produces the same type of external response as the homogeneous layer is that our inhomogeneity is invariant with respect to the x, y coordinates of the plane occupied by each face of the layer, i.e., our inhomogeneity varies only with respect to the z coordinate perpendicular to this plane. Such a model of inhomogeneity is not very different from that of [10] consisting of a row of cylinders and has been shown in the past to be useful for characterizing the modes of a structure containing a pseudo-planar heterogeneity [19]. Consequently, it is quite easy to simulate the data very precisely for both types of layers and eliminate two of the sources (i.e., scattering and data noise due to computational error when the data is simulated) of model

discordance mentioned previously. To make the IP even more simple, we assume that we know precisely where the layer is situated in space (occupied by the vacumn), what exactly is its thickness, what precisely is the (angle of) incidence (necessarily normal to the plane of the layer in the NRW technique), frequency and polarization of the incident plane wave, and what precisely are the amplitudes and phases of the observed reflected and transmitted waves. Finally, the two-parameter retrieval IP will be solved both by the NRW and optimization techniques, the latter being applicable also to obliquely-incident plane waves. Thus, as stressed above, we expect to be able to retrieve, over a wide range of frequencies, the true permittivity and permeability of the homogeneous layer and the effective permittivity and permeability of the the inhomogeneous layer.

2. COMPONENTS OF THE INVERSE PROBLEM

A material body $\mathcal{B}(\mathbf{b})$, subjected to a wavelike solicitation $\mathcal{S}(\mathbf{s})$, gives rise to the observable response $\mathcal{R}_d(\mathbf{b},\mathbf{s},\mathbf{r})$, with $\mathbf{b}$ and $\mathbf{s}$ denumerable sets of the physical and geometrical properties of $\mathcal{B}$ and $\mathcal{S}$ respectively and $\mathbf{r}$ the properties of the receivers. The retrieval of subsets of $\mathbf{b}$ or of $\mathbf{s}$ from $\mathcal{R}_d$ is an IP which is usually solved by minimizing the difference (in the NRW technique, this difference is taken to be zero) between $\mathcal{R}_d$ and a trial response $\mathcal{R}_r(\mathbf{B},\mathbf{S},\mathbf{R})$ incorporating the sets of variable properties grouped into the parameter vectors $\mathbf{B}$, $\mathbf{S}$ and $\mathbf{R}$ [2, 13]. The solution to this IP is denoted by $\mathbf{B}=\widetilde{\mathbf{B}}$ and/or $\mathbf{S}=\widetilde{\mathbf{S}}$. Henceforth, we seek to retrieve only subsets of $\mathbf{b}$, so that $\mathbf{s}$ is known (i.e., $\mathbf{S}=\mathbf{s}$), and we also assume $\mathbf{r}$ is known (i.e., $\mathbf{R}=\mathbf{r}$). In our IP, the numbers of entries of $\mathbf{B}$ and $\mathbf{b}$ are not necessarily equal, nor are the entries of $\widetilde{\mathbf{B}}$ necessarily close in value or nature, to those of $\mathbf{b}$. Moreover, our response is not observed but rather simulated (also denoted by $\mathcal{R}_d$) by means of the data model $\mathcal{M}_d$ which is the mathematical-numerical apparatus required to obtain the solution $\mathcal{R}_d$ of a *forward problem*. A second, so-called retrieval, model $\mathcal{M}_r$ is the mathematical-numerical apparatus required to obtain the solution $\mathcal{R}_r$ of another forward problem. We shall be particularly interested in the case in which $\mathcal{M}_r(\mathbf{B},\mathbf{s},\mathbf{r})$ is quite different from $\mathcal{M}_d(\mathbf{b},\mathbf{s},\mathbf{r})$, due essentially to the difference in number and/or nature between the entries of $\mathbf{B}$ and $\mathbf{b}$. In this study, $\mathcal{B}$ is an inhomogeneous layer in the form of a sandwich and $\mathbf{b}=\{\boldsymbol{\mu},\boldsymbol{\epsilon},\mathbf{h}\}$, with $\boldsymbol{\mu}$ a set of permeabilities, $\boldsymbol{\epsilon}$ a set of permittivities, and $\mathbf{h}$ a set of layer thicknesses. Moreover, the solicitation is a plane wave so that $\mathbf{s}=\{\theta^i,a^i,\omega\}$, wherein θ^i is the incident angle, a^i an amplitude, $\omega=2\pi f$ the angular frequency (f the frequency which will be varied), with $\mathbf{r}=\{r_1,r_2,...,r_{n_r}\}$ denoting the angular and radial coordinates of the sensors. The observation is assumed to take place in the far-field, on both sides of the layer so that $\mathbf{r}=\{r_1,r_2\}$, whose two entries are the angles of emergence of the reflected and transmitted plane waves.

The crucial point here is that $\mathcal{M}_r$ differs from $\mathcal{M}_d$ by the fact that $\mathbf{b}=\{M,E,H\}$ corresponds to a *homogeneous* layer of the same thickness as the sandwich connected with $\mathbf{B}$, whence the fact that the multitude of parameters (all of which are assumed to be real, with $\boldsymbol{\mu}$ and $\boldsymbol{\epsilon}$ assumed to not depend on f) contained in the three vectors of $\mathbf{b}$ are reduced to the only three scalar (real or complex), possibly frequency-dependent parameters in $\mathbf{B}$.

3. THE DATA MODEL ($\mathcal{M}_d$) BOUNDARY VALUE PROBLEM

Figure 1 depicts the linear, *inhomogeneous, non-lossy, non-dispersive*, x,y-independent layer structure (sandwich) in its cross-section plane. The half-infinite regions below and above the sandwich are Ω_0 and Ω_4 respectively, filled with media $\mathfrak{m}^{[0]}$ and $\mathfrak{m}^{[4]}$. The upper and lower plane-parallel faces of the sandwich are $z=0$ and $z=-h_6$ respectively. The sandwich is composed of three homogeneous sublayers, which occupy the regions Ω_1, Ω_2, Ω_3, whose thicknesses are h_1, h_2, h_3, with $h_6=h_1+h_2+h_3$. The upper and lower plane parallel faces of the middle sublayer are $z=-h_3$ and $z=-h_5=-(h_2+h_3)$ respectively. The isotropic, homogeneous medium in Ω_j is $\mathfrak{m}^{[j]}$, described by the two real, scalar constitutive constants $\mu^{[j]}$ (permeability), $\epsilon^{[j]}$ (permittivity). The sandwich becomes a homogeneous layer when the three media in Ω_1, Ω_2, Ω_3 are identical, so that the sandwich data model applies equally well to simulate the response data of a homogenous layer. The incident plane wave propagates in Ω_0 and is associated either with the electric field e^i_y (i.e., $h^i_y=0$; the TE-polarization case) or the magnetic field h^i_y (i.e., $e^i_y=0$;

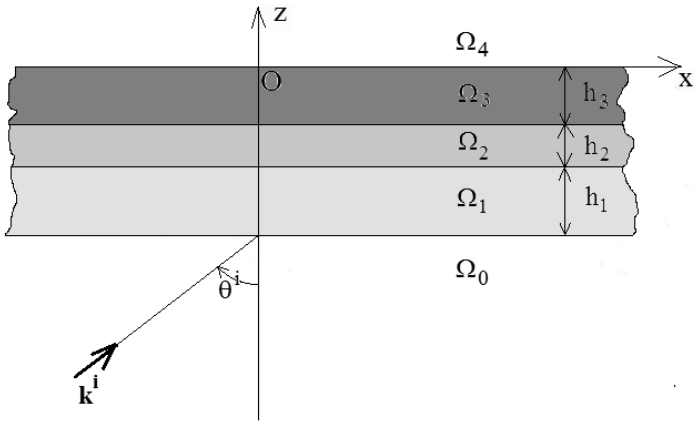

Figure 1. Scattering configuration in the sagittal plane. Normal incidence corresponds to $\theta^i = 0$.

the TM-polarization case). This wave produces a response in Ω_j to which are associated the total fields $e_y^{[j]}$ (i.e., $h_y^{[j]} = 0$) in the TE case, and $h_y^{[j]}$ (i.e., $e_y^{[j]} = 0$) in the TM case.

Let $u^{[j]}(\mathbf{x}, \omega)$ (wherein $\mathbf{x}$ is the vector, in the x-z plane, joining the origin O to the generic point (x, z)) denote the frequency domain total electric (magnetic) field in Ω_j for the TE (TM) case. Maxwell's equations give rise to:

$$u^{[j]}_{,xx}(\mathbf{x}, \omega) + u^{[j]}_{,zz}(\mathbf{x}, \omega) + (k^{[j]})^2 u^{[j]}(\mathbf{x}, \omega) = 0; \ \forall \mathbf{x} \in \Omega_j, \ j = 0, 1, 2, 3, 4, \tag{1}$$

wherein: $u_{,z} = \partial u/\partial z$, $u_{,zz} = \partial^2 u/\partial z^2$, and $k^{[j]} = \omega/c^{[j]}$, $c^{[j]} = 1/\sqrt{\mu^{[j]}\epsilon^{[j]}}$. The general solution of Eq. (1) satisfying the radiation conditions at $z \to \pm\infty$ is $u^{[j]}(\mathbf{x}, \omega) = u^{[j+]}(\mathbf{x}, \omega) + u^{[j]-}(\mathbf{x}, \omega)$, with

$$u^{[j]+}(\mathbf{x}, \omega) = a^{[j]}(\omega) \exp[i(k_x x + k_z^{[j]} z)], \quad u^{[j]-}(\mathbf{x}, \omega) = b^{[j]}(\omega) \exp[i(k_x x - k_z^{[j]} z)], \tag{2}$$

$$b^{[4]}(\omega) = 0, \quad k_x = k^{[0]} \sin\theta^i, \quad k_z^{[j]} = \sqrt{[k^{[j]}]^2 - (k_x)^2}, \quad \Re k_z^{[j]} \geq 0, \quad \Im k_z^{[j]} \geq 0; \ \forall \omega \geq 0, \tag{3}$$

and θ^i the incident angle associated with the incident plane wave $u^{[0]+} = a^{[0]}(\omega) \exp(i\mathbf{k}^i \cdot \mathbf{x})$ whose spectral amplitude (a supposedly-known function) is $a^{[0]}$. The eight unknown coefficients $b^{[j]}$; $j = 0, 1, 2, 3$ and $a^{[j]}$; $j = 1, 2, 3, 4$ are obtained from the eight transmission conditions on the four interfaces $z_1 = -h_6$, $z_2 = -h_5$, $z_3 = -h_3$, $z_4 = 0$:

$$u^{[j-1]}(x, z_j, \omega) - u^{[j]}(x, z_j, \omega) = 0, \quad f^{[j-1]} u^{[j-1]}_{,z}(x, z_j, \omega) - f^{[j]} u^{[j]}_{,z}(x, z_j, \omega) = 0; \\ \forall x \in \mathbb{R}; \quad j = 1, 2, 3, 4. \tag{4}$$

wherein $f^{[j]} = 1/\mu^{[j]}$ (TE), and $f^{[j]} = 1/\epsilon^{[j]}$ (TM). Two of these transmission conditions lead to explicit expressions of $b^{[3]}$ and $a^{[4]}$ in terms of $a^{[3]}$ and the remaining transmission conditions give rise to an easily-inverted matrix equation for the other six coefficients. Of particular interest are the reflection and transmission coefficients $b^{[0]}$ and $a^{[4]}$ respectively in the regions below, and above the inhomogeneous layer since these coefficients are what constitutes the simulated data employed further on to solve the inverse problem for both the homogeneous and inhomogeneous layers.

4. THE RETRIEVAL MODEL ($\mathcal{M}_r$) BOUNDARY VALUE PROBLEM

Figure 1, in which the three sublayers are replaced by a single layer, depicts the *homogeneous*, linear, isotropic x, y-independent layer structure (in its cross-section plane). Ω_0 and Ω_4, filled with $\mathfrak{M}^{[0]} = \mathfrak{m}^{[0]}$ and $\mathfrak{M}^{[4]} = \mathfrak{m}^{[4]}$ respectively are as previously. The *generally-dispersive, lossy*, linear, isotropic, homogeneous layer occupies, in the cross-section plane, the region Ω whose upper and lower plane

parallel faces are $z = 0$ and $z = -H = -h_6$ respectively. The constitutive parameters of the medium $\mathfrak{M}$ in the layer are the two complex functions (of the angular frequency ω) $M(\omega) = M'(\omega) + iM''(\omega)$ (permeability), and $E(\omega) = E'(\omega) + iE''(\omega)$ (permittivity). The layer is again solicited by a plane wave propagating in Ω_0 with which is associated either the electric field E_y^i (i.e., $H_y^i = 0$; TE-case) or the magnetic field H_y^i (i.e., $E_y^i = 0$; TM case). With $U^{[j]}(\mathbf{x}, \omega)$ denoting the frequency domain total electric (magnetic) fields in Ω_j ; $j = 0, 4, 6$ respectively for the TE (TM) case, and $\Omega_6 = \Omega$, the wave equations are (1) in which $U^{[j]}, K^{[j]}$ replace $u^{[j]}, k^{[j]}$ with $K^{[j]} = \omega/C^{[j]}$, $C^{[j]} = 1/\sqrt{M^{[j]}/E^{[j]}}$, $M^{[6]} = M$, $E^{[6]} = E$. As previously, we find: $U^{[j]}(\mathbf{x}, \omega) = U^{[j+]}(\mathbf{x}, \omega) + U^{[j]-}(\mathbf{x}, \omega)$, with:

$$U^{[j]+}(\mathbf{x}, \omega) = A^{[j]}(\omega) \exp[i(K_x x + K_z^{[j]} z)], \quad U^{[j]-}(\mathbf{x}, \omega) = B^{[j]}(\omega) \exp[i(K_x x - K_z^{[j]} z)], \tag{5}$$

$$B^{[4]}(\omega) = 0, \quad K_x = K^{[0]} \sin \Theta^i, \quad K_z^{[j]} = \sqrt{[K^{[j]}]^2 - (K_x)^2}, \ \Re K_z^{[j]} \geq 0, \ \ \Im K_z^{[j]} \geq 0; \ \forall \omega \geq 0, \tag{6}$$

whereas Θ^i is the incident angle associated with the incident plane wave $U^{[0]+} = A^{[0]}(\omega) \exp(i\mathbf{K}^i \cdot \mathbf{x})$ whose spectral amplitude (a supposedly-known function) is $A^{[0]}$. The four unknown coefficients $B^{[j]}$; $j = 0, 6$ and $A^{[j]}$; $j = 6, 4$ are obtained from the four transmission conditions on the two interfaces $z_3 = -H_6 = -H$, $z_5 = 0$ as previously. The reflection and transmission coefficients $B^{[0]}$ and $A^{[4]}$ respectively in the regions below and above the homogeneous layer are given in Section 5.

5. THE NRW METHOD FOR THE RETRIEVAL OF THE EFFECTIVE PERMITTIVITY AND EFFECTIVE PERMEABILITY

The NRW method [10, 18] provides explicit, exact solutions to the inverse problem of the simultaneous retrieval of M and E from the observed reflection and transmission functions $B^{[0]}$ and $A^{[4]}$ in the case $K^{[4]} = K^{[0]}$ and $\Theta^i = 0$, i.e., the two media adjoining the homogenized layer are identical, and the plane wave strikes the layer at normal incidence. Note that the NRW method treats the layer as being homogeneous, but the observed reflection and transmission functions can be those of either an inhomogeneous or homogeneous layer. The explicit solutions of the boundary-value problem of Section 4 are (in the notation of [1])

$$B^{[0]} = -A^{[0]}(E_{06}^-)^2 S_{11}, \quad A^{[4]} = A^{[0]} E_{06}^- S_{21}, \quad E_{jk}^{\pm} = \exp(\pm i K_z^{[j]} H_k), \tag{7}$$

wherein:

$$S_{11} = \Gamma \left(\frac{1 - T^2}{1 - \Gamma^2 T^2} \right), \quad S_{21} = T \left(\frac{1 - \Gamma^2}{1 - \Gamma^2 T^2} \right), \quad \Gamma = \frac{G^{[6]} - G^{[0]}}{G^{[6]} + G^{[0]}}, \quad T = E_{66}^+, \tag{8}$$

and $G^{[j]} = G_E^{[j]} = K_z^{[j]}/M^{[j]}$ in the TE case, whereas $G^{[j]} = G_H^{[j]} = K_z^{[j]}/E^{[j]}$ in the TM case.

Next consider the problem at hand of the retrieval of $M = M^{[6]}$ and $E = E^{[6]}$ from S_{11} and S_{21}. It can be shown [1] that T admits two solutions

$$T_{\pm} = -\frac{(S_{11} + S_{21}) - \Gamma_{\pm}}{1 - \Gamma_{\pm}(S_{11} + S_{21})}, \quad \Gamma_{\pm} = L \pm \sqrt{L^2 - 1}, \quad L = \frac{S_{11}^2 - S_{21}^2 + 1}{2S_{11}}. \tag{9}$$

In the assumed case of normal incidence, $K_z^{[6]} = K^{[6]}$ and $T_{\pm} = \exp(iK_{\pm}^{[6]} H_6)$, with $K_{\pm}^{[6]} = K_{\pm}^{[6]'} + iK_{\pm}^{[6]''}$, $T_{\pm} = T'_{\pm} + iT''_{\pm}$ so that

$$K_{\pm}^{[6]''} = -\frac{1}{h_6} \ln \left(\sqrt{T_{\pm} T_{\pm}^*} \right), \quad K_{m\pm}^{[6]'} = -\frac{1}{h_6} \left[\arctan \left(\frac{T''_{\pm}}{T'_{\pm}} \right) + m\pi \right]; \ m = 0, \pm 1, \pm 2, \ldots. \tag{10}$$

with $*$ denoting the complex conjugate. Also, let

$$Z^{[6]} = \sqrt{\frac{M}{E}}. \tag{11}$$

and recall that

$$C^{[6]} = \frac{\omega}{K^{[6]}} = \sqrt{\frac{1}{ME}}. \tag{12}$$

In the TE case, $\Gamma = \Gamma_E$, whereas in the TM case, $\Gamma = \Gamma_H$, so that

$$Z^{[6]} = Z_E^{[6]} = Z^{[0]}\left(\frac{1-\Gamma_E}{1+\Gamma_E}\right), \quad Z^{[6]} = Z_H^{[6]} = Z^{[0]}\left(\frac{1+\Gamma_H}{1-\Gamma_H}\right), \tag{13}$$

wherein $Z^{[0]} = \sqrt{\mu^{[0]}/\epsilon^{[0]}}$. It then follows that:

$$M = \frac{Z^{[6]}K^{[6]}}{\omega}, \quad E = \frac{K^{[6]}}{Z^{[6]}\omega}, \tag{14}$$

or, on account of the dependencies on the polarization and $m\pm$:

$$M_{Em\pm} = \frac{Z_{Em\pm}^{[6]}K_{Em\pm}^{[6]}}{\omega}, \quad E_{Em\pm} = \frac{K_{Em\pm}^{[6]}}{\omega Z_{Em\pm}^{[6]}};\ m = 0, \pm1, \pm2, \ldots, \tag{15}$$

$$M_{Hm\pm} = \frac{Z_{Hm\pm}^{[6]}K_{Hm\pm}^{[6]}}{\omega}, \quad E_{Hm\pm} = \frac{K_{Hm\pm}^{[6]}}{\omega Z_{Hm\pm}^{[6]}};\ m = 0, \pm1, \pm2, \ldots. \tag{16}$$

Thus, as a result of the NRW scheme, the inverse homogeneous layer problem appears to possess a doubly-infinite set of solutions at each frequency and for each polarization. To verify that a particular set $\{M, E\} = \{M_{Em\pm}, E_{Em\pm}\}$ or $\{M, E\} = \{M_{Hm\pm}, H_{Em\pm}\}$ is a valid solution of the inverse problem, we must show that it enables the regeneration of the data S_{11}, S_{21} for all $\omega = 2\pi f$. To do this, we carry out the preceding operations, at each frequency, in reverse order and reject the $\{M_{m\pm}, E_{m\pm}\}$ for which the reconstructed reflection coefficient does not equal S_{11} or the reconstructed transmission coefficient does not equal S_{21}.

6. COMPUTATIONAL PROCEDURES

6.1. Data

We shall employ two types of (complex) data:

choice 1: $\mathcal{R}_{d1}(\omega) = b^{[0]}(\omega, \theta^i)$, $\mathcal{R}_{d2}(\omega) = a^{[4]}(\omega, \theta^i)$;

choice 2: $\mathcal{R}_{d1}(\omega) = b^{[0]}(\omega, \theta_1^i)$, $\mathcal{R}_{d2}(\omega) = a^{[4]}(\omega, \theta_1^i)$, $\mathcal{R}_{d3}(\omega) = b^{[0]}(\omega, \theta_2^i)$, $\mathcal{R}_{d4}(\omega) = a^{[4]}(\omega, \theta_2^i)$, $\ldots$, $\mathcal{R}_{dn_r-1}(\omega) = b^{[0]}(\omega, \theta_{n_r/2}^i)$, $\mathcal{R}_{dn_r}(\omega) = a^{[4]}(\omega, \theta_{n_r/2}^i)$.

The first choice is made for the NRW technique; we shall also use it in the optimization method. The second choice stems from the requirement [15] that the constitutive properties of a homogenized layer be independent of the angle of incidence of the plane wave solicitation; we shall employ it in the optimization method in order to reduce the number of candidate solutions of the IP.

6.2. Priors, Unknown Parameters and To-Be-Retrieved Parameter Functions

In Section 2, we introduced the three true parameter sets involved in the inverse problem: $\mathbf{b}, \mathbf{s}, \mathbf{r}$. We also wrote that $\mathbf{s}, \mathbf{r}$ were assumed to be known (they are therefore termed *priors*, which means that they are not to be retrieved) and that $\mathbf{S} = \mathbf{s}$ and $\mathbf{R} = \mathbf{r}$, so that only $\mathbf{b}$ was unknown. Hereafter, the entries of the sets $\mathbf{s}, \mathbf{r}$ are given by $\mathbf{S} = \mathbf{s} = \{\theta^i, a^i, \omega\}$, with $a^{[0]} = A^{[0]} = a^i = 1$ at all ω, and $\mathbf{R} = \mathbf{r} = \{\theta^r, \theta^t\}$, for choice 1 data ($\theta^r$, θ^t, the angles of specular reflection and transmission for incidence angle θ^i) and $\mathbf{r} = \{\theta_1^r, \theta_1^t, \theta_2^r, \theta_2^t, \ldots, \theta_{n_r/2}^r, \theta_{n_r/2}^t\}$ for choice 2 data. In the usual constitutive parameter retrieval problems, one aims at estimating one or more of the entries of $\mathbf{b}$, termed *unknown or to-be-retrieved parameters*, the other entries being priors, so that for the present sandwich characterization problem, the unknown parameters would be from one to nine of the *real, frequency-independent* entries in the set

$$\mathbf{b} = \{\boldsymbol{\mu}, \boldsymbol{\epsilon}, \mathbf{h}\} = \left\{\mu^{[1]}, \mu^{[2]}, \mu^{[3]}, \epsilon^{[1]}, \epsilon^{[2]}, \epsilon^{[3]}, h_1, h_2, h_3\right\}. \tag{17}$$

In Section 2, we stressed the crucial difference between the present approach and the traditional constitutive parameter retrieval approach, by the fact that the entries in the trial set $\mathbf{B}$ may be different in number and nature from those of the set $\mathbf{b}$. At present, this is manifested by the choice

$$\mathbf{B} = \{M(\omega_m), E(\omega_m); m = 1, 2, \ldots, m_\omega, H\}, \tag{18}$$

wherein $\omega_m = \omega_b + (m-1)(\frac{\omega_e - \omega_b}{m_\omega - 1})$; $m = 1, 2, \ldots, m_\omega$, it being understood that $M(\omega)$ and $E(\omega)$ are generally-*complex* functions of ω which we term the *to-be-retrieved parameter functions (of frequency)*. Note that the response functions involved in both the forward and inverse problems at a given frequency ω_1 are independent of their counterparts at frequency ω_2, whatever be ω_1 and ω_2. This means that $M(\omega), E(\omega)$ can, and should, be retrieved *frequency-by-frequency* in the interval $[\omega_b, \omega_e]$, so that *at a given frequency ω_m, there are only two (generally) complex unknowns*: $M(\omega_m), E(\omega_m)$, assuming that h is a prior and that $H = h$.

6.3. Cost Function in the Optimization Method

The basic tool of the optimization method [2, 13] is the cost function $\mathcal{K}$ which is a measure of the discrepancy between the data response(s) and the trial response(s). Our choice of cost functions (one for each frequency ω_m) is

$$\mathcal{K}(\mathbf{B}_m) = \frac{\sum_{n=1}^{n_r} \left(\mathcal{R}_{dn}(\omega_m) - \mathcal{R}_{rn}(\omega_m)\right) \left(\mathcal{R}_{dn}(\omega_m) - \mathcal{R}_{rn}(\omega_m)\right)^*}{\sum_{n=1}^{n_r} \left(\mathcal{R}_{dn}(\omega_m)\right) \left(\mathcal{R}_{dn}(\omega_m)\right)^*}; \quad m = 1, 2, \ldots, m_\omega, \tag{19}$$

wherein $\mathcal{R}_{dn}(\omega_m) = \mathcal{R}_d(\omega_m, \mathbf{b}, \mathbf{s}, r_n)$ and $\mathcal{R}_{rn}(\omega_m) = \mathcal{R}_r(\omega_m, \mathbf{B}_m, \mathbf{s}, r_n)$, $\mathbf{B}_m = \{M(\omega_m), E(\omega_m), h\}$. Note that $n_r = 2$ for choice 1 data and $n_r \geq 4$ for choice 2 data.

6.4. Candidate Solutions of the Inverse Problem Obtained by Minimization of the Cost Function

In the optimization scheme, the inversion proceeds by searching (at each ω_m) for the (relative and global) minima of the cost function $\mathcal{K}$ within: either a two-dimensional (2D) search space of trial parameters $M'_m = \Re M(\omega_m)$ ($M''_m = \Im M(\omega_m) = 0$ implicitly), $E'_m = \Re E(\omega_m)$, ($E''_m = \Im E(\omega_m) = 0$ implicitly) or a four-dimensional (4D) search space of trial parameters $M'_m = \Re M(\omega_m)$, $M''_m = \Im M(\omega_m)$, $E'_m = \Re E(\omega_m)$, $E''_m = \Im E(\omega_m)$. The 2D search space is such that $M'_m \in [\underline{M'_m}, \overline{M'_m}]$, $E'_m \in [\underline{E'_m}, \overline{E'_m}]$. The 4D search space is such that $M'_m \in [\underline{M'_m}, \overline{M'_m}]$ $M''_m \in [\underline{M''_m}, \overline{M''_m}]$, $E'_m \in [\underline{E'_m}, \overline{E'_m}]$, $E''_m \in [\underline{E''_m}, \overline{E''_m}]$.

In the 2D problem, the choice of $\underline{M'_m}, \overline{M'_m}$ and $\underline{E'_m}, \overline{E'_m}$ is dictated by a priori knowledge one may have of the solution to the inverse problem such as is provided by mixing formulae (see Section 6.5). The same holds true for the 4D problem. The hypervolume of the search space is usually larger in the case of an inhomogeneous material because the effective dynamic properties of the latter are generally less-well known a priori than those of a homogeneous material. Moreover, the larger is the search space, the more likely one will encounter relative minima. A severe restriction of the size of the search space is not a remedy to this problem since it might entail the elimination of significant candidate retrievals. Also, the larger the difference between the homogenized layer and the sandwich, the more difficult it is to find well-defined troughs in the cost function, which often means that many solutions are equally likely. If possible, as is the case in 2D problems (which is a good reason for treating them first), one should take a look at the graphs of the cost function to understand their topography. Whatever the dimension of the problem, the adopted solution, at each frequency, is chosen to correspond to the global minimum of the cost function in the last selected search space. This guarantees uniqueness, but does not mean that relative minima are absent in the cost functional at apparently-plausible locations.

6.5. Mixture Models to Furnish a Priori Estimations of the Properties of the Homogenized Layer

Consider the sandwich in its sagittal plane. The total area per unit length in the x direction of the sandwich is h. The area per unit length of the j-th sublayer is h_j. The filling factor (of the sublayer area with respect to the total area) is $\phi_j = h_j/h$, which varies between 0 (no sublayer) and 1 (sublayer

occupying the whole sandwich). The general mixing formula [14], thought to be valid at low frequencies only, takes the following particular forms (on account of the assumed lossless nature of the sublayers of the sandwich):

$$M' \approx M'_{\|} = \mu^{[1]}\phi_1 + \mu^{[2]}\phi_2 + \mu^{[3]}\phi_3, \quad M'' \approx M''_{\|} = 0, \tag{20}$$

$$E' \approx E'_{\|} = \epsilon^{[1]}\phi_1 + \epsilon^{[2]}\phi_2 + \epsilon^{[3]}\phi_3, \quad E'' \approx E''_{\|} = 0, \tag{21}$$

or, alternatively:

$$(M')^{-1} \approx (M'_{\perp})^{-1} = (\mu^{[1]})^{-1}\phi_1 + (\mu^{[2]})^{-1}\phi_2 + (\mu^{[3]})^{-1}\phi_3, \quad (M'')^{-1} \approx (M''_{\perp})^{-1} = \infty, \tag{22}$$

$$(E')^{-1} \approx (E'_{\perp})^{-1} = (\epsilon^{[1]})^{-1}\phi_1 + (\epsilon^{[2]})^{-1}\phi_2 + (\epsilon^{[3]})^{-1}\phi_3, \quad (E'')^{-1} \approx (E''_{\perp})^{-1} = \infty, \tag{23}$$

Eqs. (20)–(21) and (22)–(23) are the so-called parallel and series (respectively) versions of more general mixing formulae [14]. Note that neither the frequency nor other parameters of the problem enter into these mixing formulae. Moreover, the latter show that the three constitutive parameters are not related one to the other. We shall compare the predictions of the parallel and series (red horizontal lines in the graphs) formulae to the the estimations of the properties of the homogenized layer obtained by the 2D and 4D optimization schemes.

6.6. True Parameters

In all cases, we chose: $\mu^{[j]} = \mu_0$, $\epsilon^{[j]} = \epsilon_0$; $j = 0, 4$, with μ_0 and ϵ_0 the permeability and permittivity in the vacumn. The units of frequencies f in the graphs are GHz. The true relative parameters of the homogeneous layer are: $\mu_r^{[6]} = \mu^{[6]}/\mu_0 = 2$ and $\epsilon_r^{[6]} = \epsilon^{[6]}/\epsilon_0 = 2.25$, with $h_6 = 0.012\,\mathrm{m}$, so that $k^{[6]}h_6$ varies from 0.5332 to 2.6658 when f varies from 1 to 5 GHz. The fixed true relative parameters of the three sublayer sandwich are: $\mu_r^{[j]} = 2$ and $\epsilon_r^{[j]} = 2.25$; $j = 1, 3$ with $h_1 = 0.004\,\mathrm{m}$, $h_2 = 0.006\,\mathrm{m}$, $h_3 = 0.004\,\mathrm{m}$ (all fixed). The variable relative parameters $\mu_r^{[2]}$, $\epsilon_r^{[2]}$ of the central sublayer of the sandwich are as indicated in the figure captions. The angle of incidence is 0° relative to all the NRW results and most of the optimization results, and varies between 0° and 40° in 10° steps in the remainder of the optimization results. The polarization in the graphs is TM (index H, whereas in the TE case the index is E) since we found that $M_{Em_\pm} = M_{Hm_\mp}$ and $E_{Em\pm} = E_{Hm\mp}$.

7. RETRIEVALS OBTAINED VIA THE NRW SCHEME FOR $\theta^I = 0°$

In all the following graphs, the horizontal red lines represent the parallel and series mixture model solutions which usually nearly coincide.

7.1. Unsorted and Sorted Retrievals

The (sorting) method for distinguishing between a valid and invalid solution was described at the end of Section 5. In Figs. 2–3, the green symbols represent the unsorted NRW solutions and those with central blue points the sorted (i.e., valid) solutions.

We note that at least two valid solutions exist at each frequency (non-uniqueness) and that one of these is nearly coincident with the mixture model solutions at low frequencies. Furthermore, in what appear as continuous branches, the value of m abruptly changes at certain frequencies and at these frequencies other branches start to make their appearance. Although the general pattern of inhomogeneous (IL) and homogeneous layer (HL) solutions appear to be quite similar, notably concerning the non-uniqueness, there are notable differences: (a) in the HL case, there are no signs of Fabry-Perot resonances (FBR) contrary to the IL case, (b) in the HL case, at least one branch coincides with the true solution (which also coincides with the mixture model solutions, (c) the imaginary parts of M and E are nil (actually very small due to numerical error) in the HL case, contrary to the IL case. This means that the inhomogeneity induces an apparent dissipation (or perhaps amplification) when the layer is viewed as an effective medium.

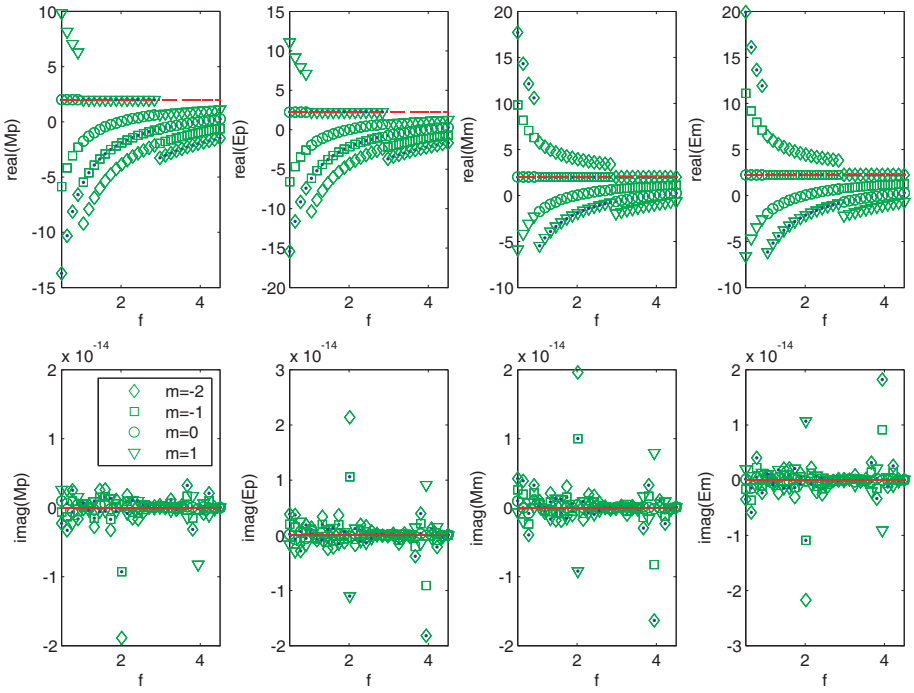

Figure 2. Candidate solutions obtained by the NRW scheme for $m = -2, -1, 0, 1$ as a function of frequency f. Mp, Mm, Ep, Em, mean M_{Hm+}, M_{Hm-}, E_{Hm+}, E_{Hm-} respectively. $\mu_r^{[2]} = 2.0$, $\epsilon_r^{[2]} = 2.25$: this is the HL case in which the totality of the layer is filled with the same material.

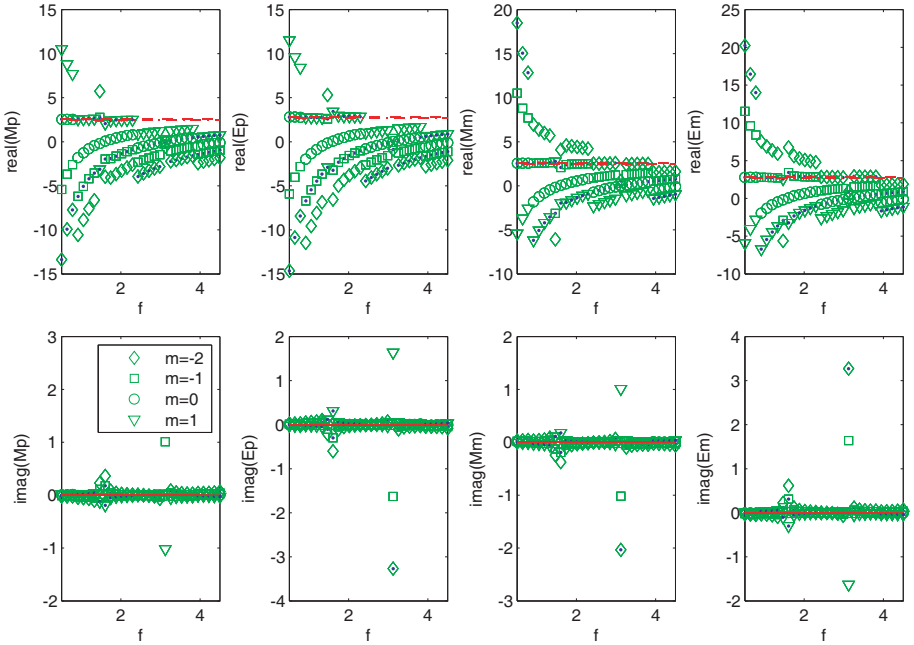

Figure 3. Same types of graphs as in Fig. 2. $\mu_r^{[2]} = 3.1$, $\epsilon_r^{[2]} = 3.35$: this is an IL case in which the central sublayer is different from the other two sublayers.

7.2. Sorted Retrievals Only

In Figs. 4–11, we depict the sorted (valid) retrievals (represented by blue points as previously) for a fixed value of m. We note that that only two such retrievals (corresponding to $m+$ and $m-$) exist for

a given m at a given frequency. In the HL case, one of these retrievals coincides with the true solution and in the IL case it is the solution closest to the mixture model prediction. *More remarkably, in both the HL and IL cases, the other solution corresponds to simultaneously-negative M' and E' in certain frequency intervals.* In other frequency intervals, this solution corresponds to simultaneously-positive M' and E'. The zooms in Figs. 10–11 show clearly the resonant nature of the $m = 1$ solution in the neighborhood of (what appears to be the Fabry-Perot frequency) $f \approx 1.6$. In this neighborhood, the real parts of M and E both switch from positive to negative values or vice-versa, this being reminiscent of what has been found (for either or both M' and E', usually via the NRW scheme) for other types of IL [3, 6, 8, 11, 16, 20].

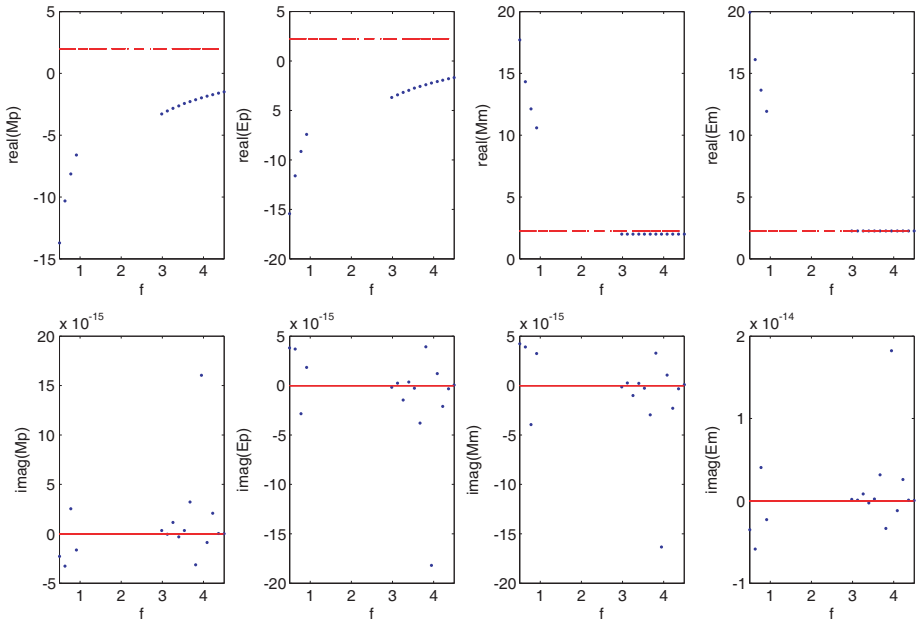

Figure 4. Valid solutions for fixed $m = -2$ as a function of f.

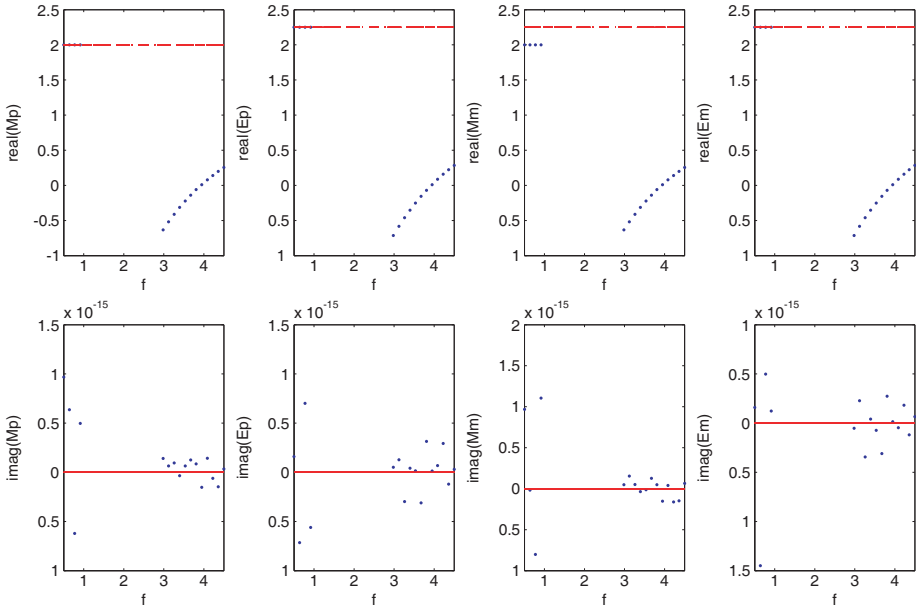

Figure 5. Valid solutions for fixed $m = 0$ as a function of f.

7.2.1. A HL Case: $\mu_r^{[2]} = 2$, $\epsilon_r^{[2]} = 2.25$

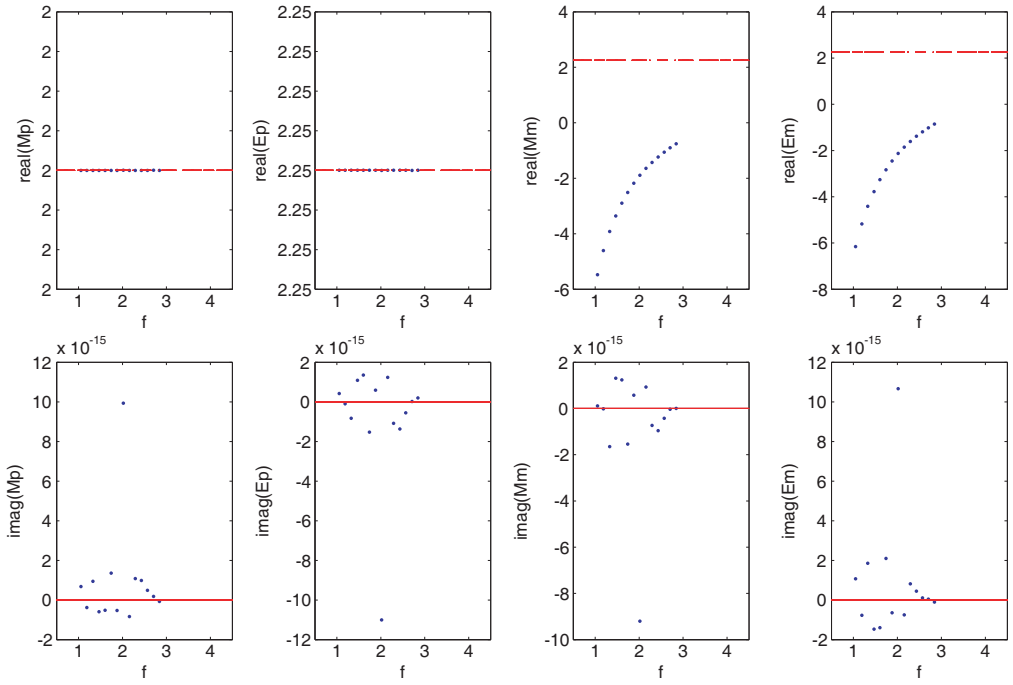

Figure 6. Valid solutions for fixed $m = 1$ as a function of f.

7.2.2. An IL Case: $\mu_r^{[2]} = 3.1$, $\epsilon_r^{[2]} = 3.35$

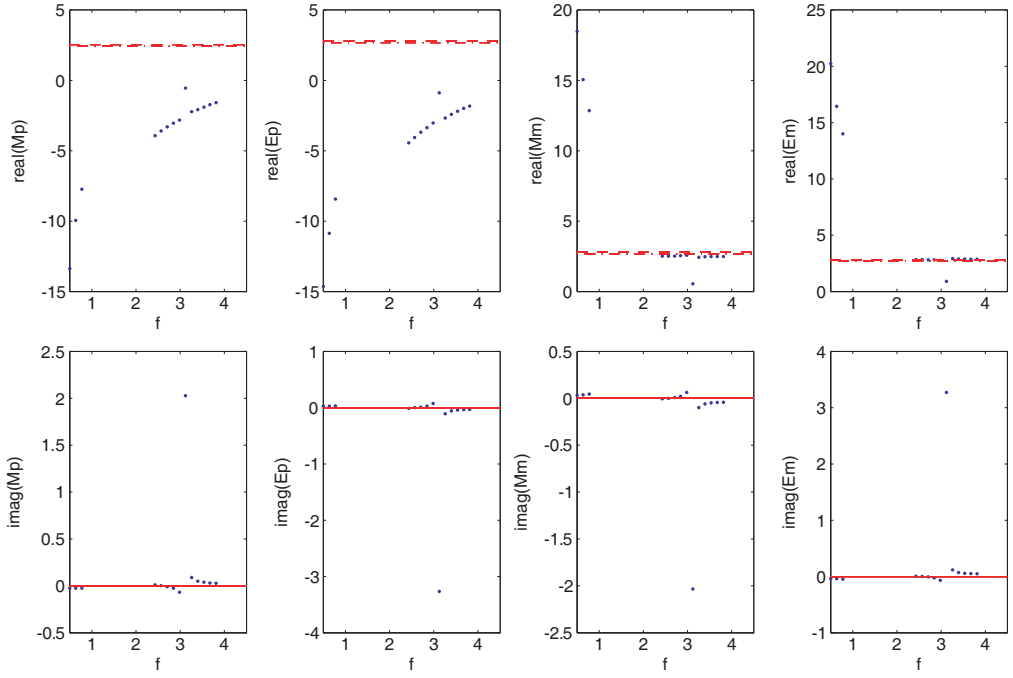

Figure 7. Valid solutions for fixed $m = -2$ as a function of f.

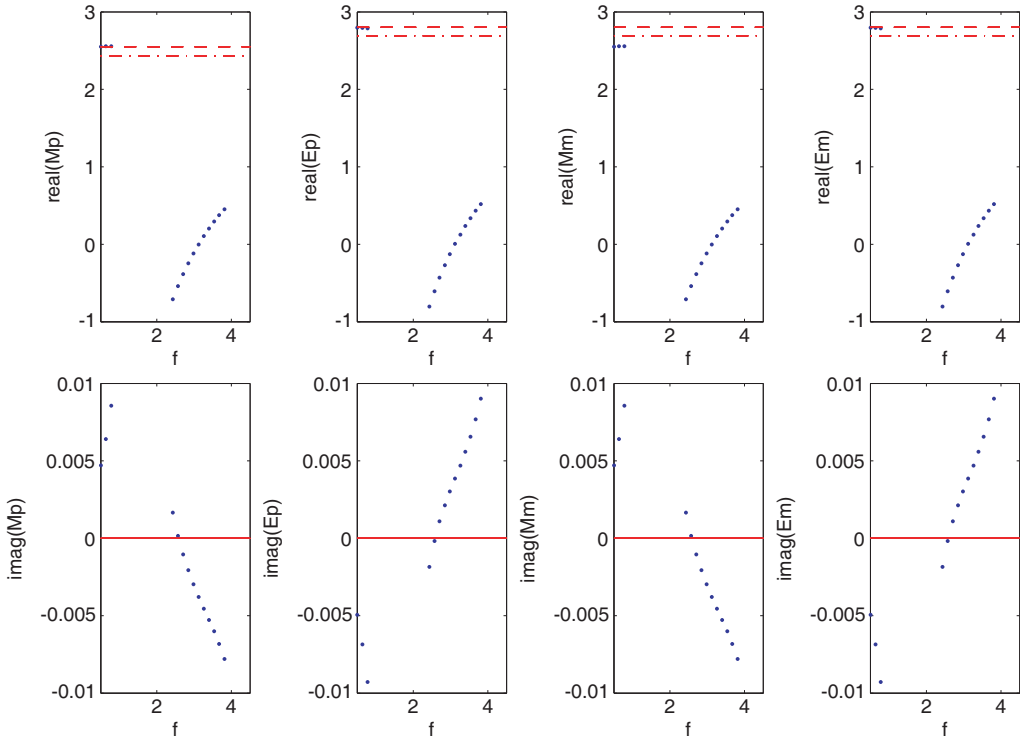

Figure 8. Valid solutions for fixed $m = 0$ as a function of f.

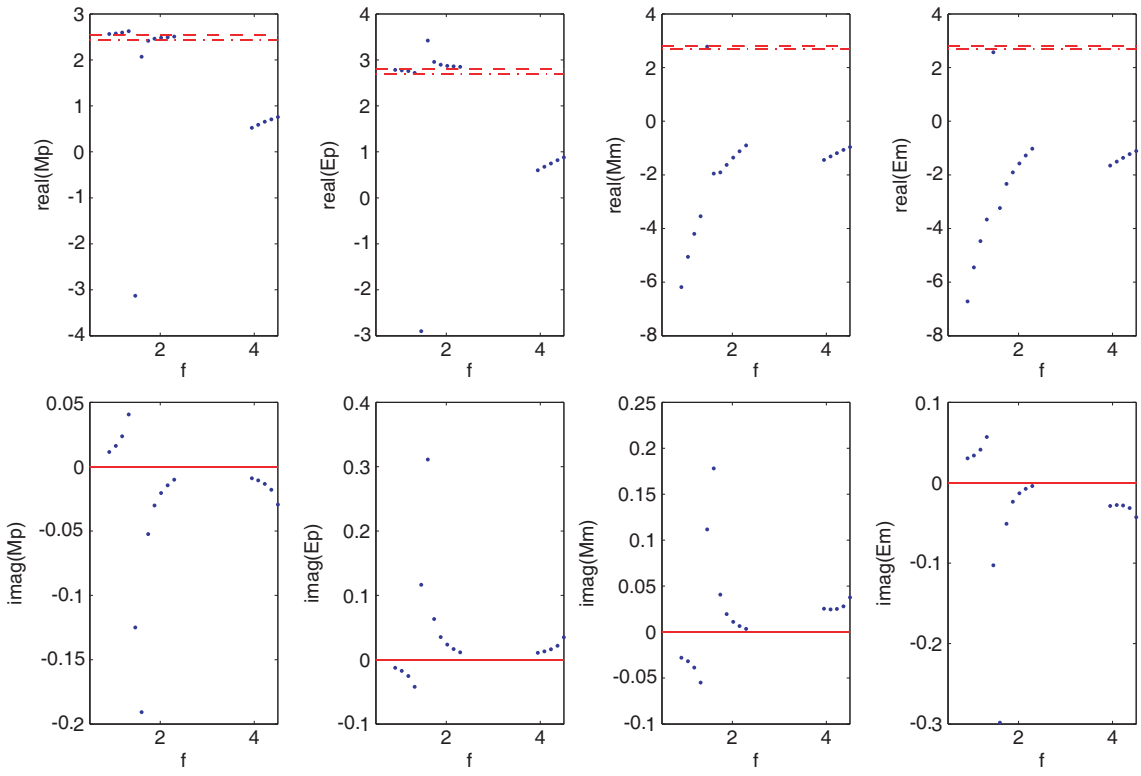

Figure 9. Valid solutions for fixed $m = 1$ as a function of f.

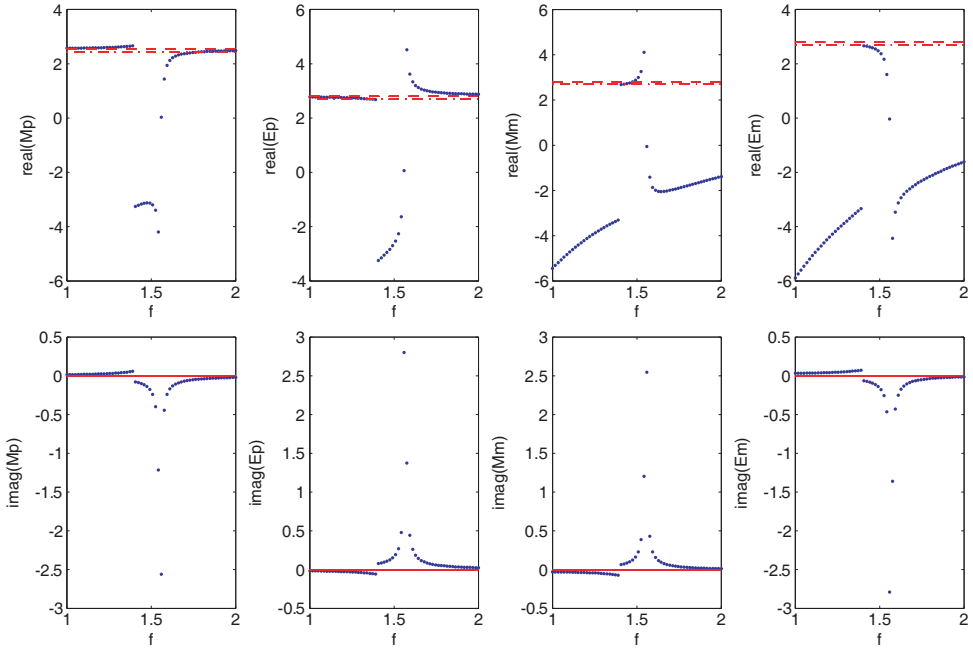

Figure 10. Zoom of Fig. 9.

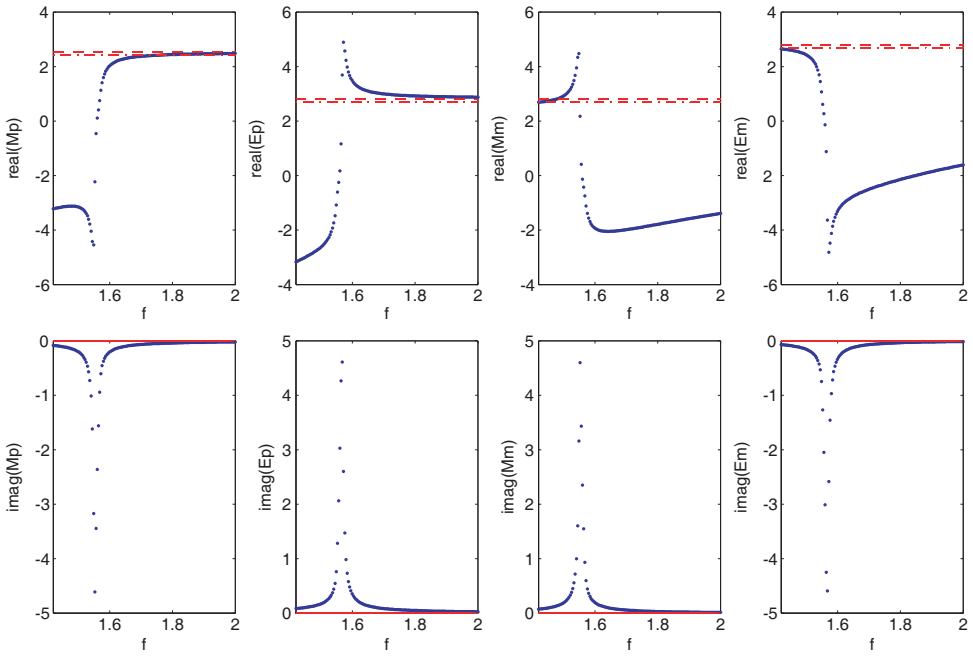

Figure 11. Super zoom of Fig. 9.

8. NUMERICAL RESULTS RELATIVE TO THE RETRIEVALS OBTAINED BY THE OPTIMIZATION SCHEME

In Figs. 12–19, the sizes of the search spaces are voluntarily chosen to be very large since the inhomogeneous nature of the layer has an incidence on the values of the retrieved effective parameters that is not known a priori (i.e., these values may be quite different from the mixture model predictions). Large search spaces means lengthy computations so that it is important to find out if it is possible to

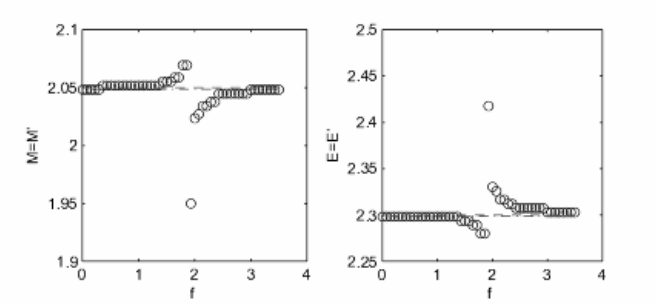

Figure 12. 2D optimization. TM polarization. $\theta^i = 0°$. $\mu_r^{[2]} = 2.1$, $\epsilon_r^{[2]} = 2.35$. The horizontal lines are relative to the mixture model predictions whereas the circles are relative to the optimization retrievals.

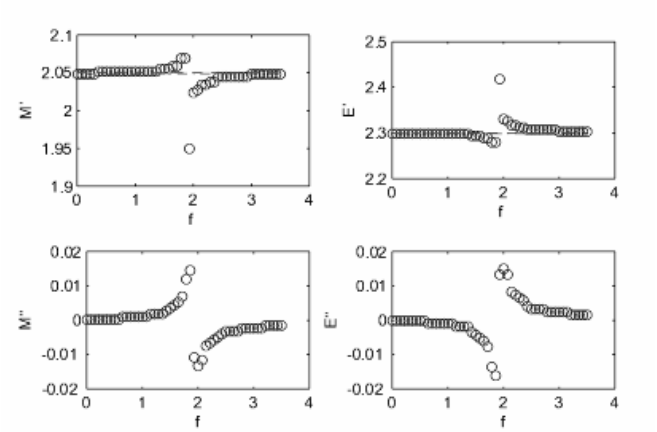

Figure 13. 4D optimization. TM polarization. $\theta^i = 0°$. $\mu_r^{[2]} = 2.1$, $\epsilon_r^{[2]} = 2.35$. Same meaning of the symbols as in previous figure.

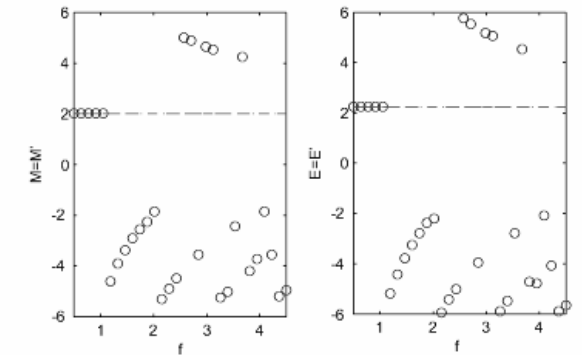

Figure 14. $n_r = 2$. $\theta^i = 0°$.

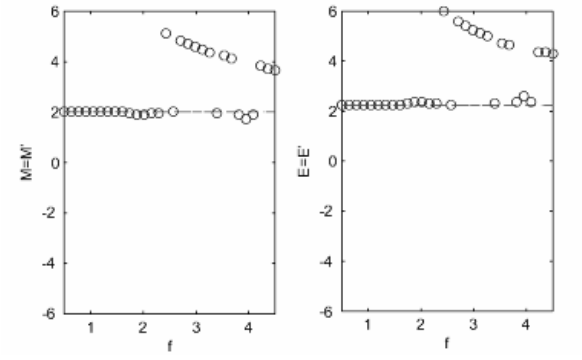

Figure 15. $n_r = 6$. $\theta^i = 0°, 10°, 20°$.

reduce the dimensions of the search spaces in order to reduce the computational burden. This is done in Section 8.1.

8.1. Comparison of 2D to 4D Optimization Results

Figure 12 shows a 2D optimization, i.e., for the retrieval of $M'(\omega)$ and $E'(\omega)$, it is assumed that $M''(\omega) = 0$ and $E''(\omega) = 0$. This figure is similar to what is found in [4] wherein observed (instead of synthetic) data are used for the retrievals. Fig. 13 shows a 4D optimization, i.e., for the retrieval of $M'(\omega)$, $M''(\omega)$, $E'(\omega)$ and $E''(\omega)$. One observes that the 2D optimization scheme leads to the same results (even in the vicinity of the Fabry-Perot resonance) for $M'(\omega)$ and $E'(\omega)$ as the 4D optimization scheme which is why we obtain the remaining retrievals by the 2D optimization scheme.

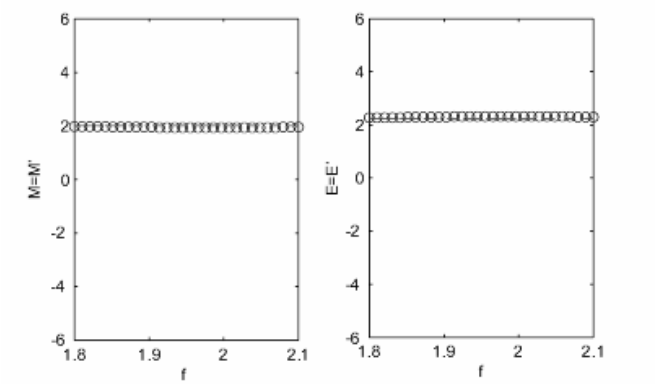

Figure 16. $n_r = 10$. $\theta^i = 0°, 10°, 20°, 30°, 40°$.

8.2. 2D Optimization Scheme Results to Determine Whether the Retrievals Can Be Made to Be Independent of the Incident Angle

Figures 14–19 encompass the results of 2D optimizations: Figs. 14–16 for a HL and Figs. 17–19 for an IL. The purpose of these figures, in which the polarization is TM, is to show how the results evolve as a function of the (number $n_r/2$ of) angles of incidence, it being recalled that the notion of effective medium implies independence of the effective properties with respect to θ^i. The employed optimization procedure is as explained in Section 6.3, for $n_r/2$ data couples (for the reflectivity and transmissivity) (see Section 6.1).

We note that for both the IL and HL, the pattern is the same as the NRW retrievals when $n_r = 2$ and $\theta^i = 0°$, evocative of non-uniqueness and the possibility of retrievals for which both M' and E' are simultaneously negative. However (again for both the IL and HL), when n_r is increased, first the negative retrievals disappear, followed by the disappearance of the positive retrievals that are very different from the mixture model predictions. For large-enough n_r, only the retrievals closest to the mixture model predictions remain, this being true for both the IL and HL (although the IL retrievals are slightly dispersive and resonant in the vicinity of what appear to be Fabry-Perot frequencies). This suggests that the only retrieved effective (or true in the case of a homogeneous layer) properties, compatible with the requirement of independence with respect to the incident angle, are those closest to the mixture model predictions and these retrievals are unique at all frequencies. Thus, the simultaneously-negative M' and E' retrievals obtained by the NRW scheme, as well as by the optimization scheme for $n_r = 2$ and $\theta^i = 0°$, are found, by the optimization scheme, to be incompatible with independence of the properties of the effective layer.

8.2.1. HL for Which $\mu^{[2]} = 2$, $\epsilon^{[2]} = 2.25$; Effect of Varying the Incident Angles

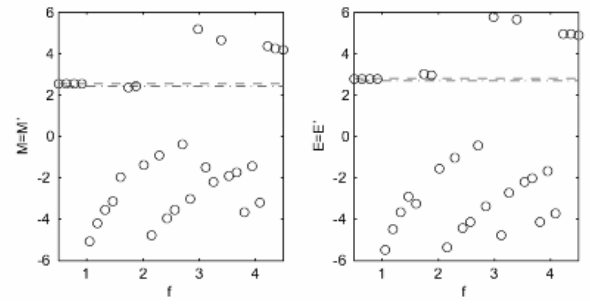

Figure 17. $n_r = 2$. $\theta^i = 0°$.

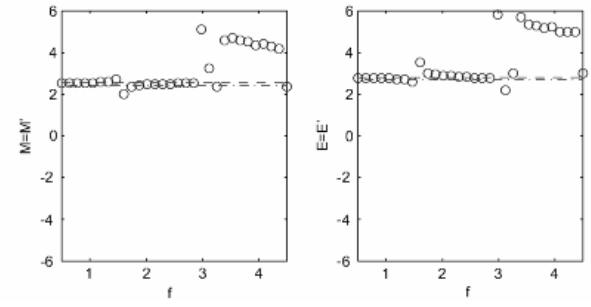

Figure 18. $n_r = 6$. $\theta^i = 0°, 10°, 20°$.

8.2.2. IL for Which $\mu^{[2]} = 3.1$, $\epsilon^{[2]} = 3.35$; Effect of Varying the Incident Angles

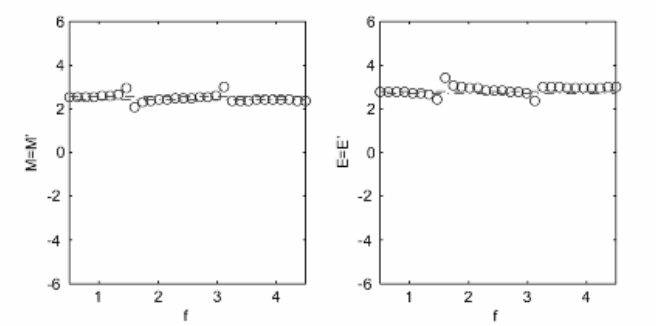

Figure 19. $n_r = 10$. $\theta^i = 0°, 10°, 20°, 30°, 40°$.

9. CONCLUSIONS

We applied both the NRW and optimization schemes to inhomogeneous (IL) as well as homogeneous (HL) layers, since the inverse problem is the same for both IL and HL, namely to retrieve the properties of a homogenous layer (homogenized in the IL case); what changes is the data, which is that of the response of a homogeneous layer for the HL and that of the response of an inhomogeneous layer for the IL.

The NRW scheme was shown to be inadapted for finding out whether simultaneous $M' < 0$ and $E' < 0$ are properties that are independent of the angle of incidence, as they should be if the retrieved properties are actually effective properties of the homogenized medium in the layer.

It was found that the numerical optimization scheme produces the same retrievals as the rigorous NRW scheme in the only case (normal incidence) in which both can be compared, and since there is no reason why the optimization scheme should change its nature for other incident angles, it can be considered to be producing correct retrievals for other angles of incidence as well.

Since the optimization scheme shows that the effective properties of the IL are unique (at each frequency) and those closest to the effective medium predictions (thus far-removed from situations in which $M' < 0$ and $E' < 0$ simultaneously), one might ask how these effective properties differ from those of a HL. This is an important question and our answer (which is only partial since we have not analyzed ordinary metamaterials) is that the IL (contrary to the HL) gives rise to temporal dispersion (anomalous in the vicinity of the Fabry-Perot frequencies, analogous to retrieval instability in the language of inversion theory [5]) and attenuation in the effective parameters M and E even when the component media of the inhomogeneous layer are non-dispersive and non-lossy. It is obvious that this feature is strongly tied up with the process of parameter inversion itself and the concept of model discordance discussed in Section 1 since it does not occur when there is no model discordance (i.e., the case in which the data is that of a HL and the retrieval model is that of a HL of the same thickness submitted to the same solicitation).

Our IL is different from those ordinarily considered as metamaterials, in which the properties of the former are not variable (as those of the latter which are usually periodic) with respect to the x, y coordinates (when each face of the layer occupies a x-y plane). Thus, the retrievals found herein do not necessarily apply to the ordinary metamaterials. Nevertheless, since the optimization scheme we employ can also be applied to these metamaterials, and since this scheme enabled us to uncover the fact that the exotic properties of simultaneous $M' < 0$ and $E' < 0$ are incompatible with the independence of these properties with respect to θ^i, we suggest that the optimization scheme (rather than the NRW) is employed in the future to retrieve the effective material properties of ordinary metamaterials, notably to find out whether these properties are really those suggested by the NRW scheme.

REFERENCES

1. Barroso, J. J. and A. L. De Paula, "Retrieval of permittivity and permeability of homogeneous materials from scattering parameters," *Journal of Electromagnetic Waves and Applications*, Vol. 24, No. 11, 1563–1574, July 2010.
2. Chambouleyron, I. and J. M. Martinez, "Optical properties of dielectric and semiconductor thin films," *Handbook of Thin Films Materials*, Vol. 3, Nalwa H. S. (ed.), Academic Press, New York, 2001.
3. Chen, X., T. M. Grzegorczyk, B.-I. Wu, J. Pacheco, Jr., and J. A. Kong, "Robust method to retrieve the constitutive effective parameters of metamaterials," *Phys. Rev. E*, Vol. 70, 016608, 2004.
4. De Paula, A. L., M. C. Rezende, and J. J. Barroso, "Experimental measurements and numerical simulation of permittivity and permeability of Teflon in X band," *J. Aerosp. Technol. Manag.*, Vol. 3, 59–64, Sao Jose dos Campos, 2011.
5. Hadamard, J., *Lectures on Cauchy's Problem in Linear Partial Differential Equations*, Yale University Press, New Haven, 1923.
6. Liu, X.-X. and A. Alu, "Generalized retrieval method for metamaterial constitutive parameters based on a physically-driven homogenization approach," *Phys. Rev. B*, Vol. 87, 235136, 2013.
7. Liu, X.-X., D. A. Powell, and A. Alu, "Correcting the Fabry-Perot artifacts in metamaterial retrieval procedures," *Phys. Rev. B*, Vol. 84, 235106, 2011.
8. Markos, P. and C. M. Soukoulis, "Transmission properties and effective electromagnetic parameters of double negative metamaterials," *Optics Expr.*, Vol. 11, 649–661, 2003.
9. Menzel, C., T. Paul, C. Rockstuhl, T. Pertsch, S. Tretyakov, and F. Lederer, "Validity of effective material parameters for optical fishnet metamaterials," *Phys. Rev. B*, Vol. 81, 035320, 2010.
10. Nicolson, A. M. and G. Ross, "Measurement of the intrinsic properties of materials by time-domain techniques," *IEEE Trans. Instrum. Meas.*, Vol. 19, 377–382, 1970.
11. O'Brien, S. and J. B. Pendry, "Photonic band-gap effects and magnetic activity in dielectric composites," *J. Phys. Condens. Matter*, Vol. 14, 4035–4044, 2002.
12. Ogam, E., Z. E. A. Fellah, and P. Baki, "The inverse problem of acoustic wave scattering by an air-saturated poroelastic cylinder," *J. Acoust. Soc. Am.*, Vol. 133, No. 3, 1443–1457, 2013.
13. Seal, M. D., M. W. Hyde, IV, and M. J. Havrilla, "Nondestructive complex permittivity and permeability extraction using a two-layer dual-waveguide probe measurement geometry," *Progress In Electromagnetics Research*, Vol. 123, 123–142, 2012.
14. Sihvola, A., "Mixing models for heterogeneous and granular Media," *Advances in Electromagnetics of Complex Media and Metamaterials*, S. Zouhdi, A. Sihvola, and M. Arsalane (eds.), Kluwer, Amsterdam, 2002.
15. Simovski, C. R. and S. A. Tretyakov, "On effective electromagnetic parameters of artificial nanostructured magnetic materials," *Photonics Nanostruct. Fundamen.*, Vol. 8, No. 4, 254–263, 2010.
16. Smith, D. R., S. Schultz, P. Markos, and C. M. Soukoulis, "Determination of effective permittivity and permeability of metamaterials from reflection and transmission coefficients," *Phys. Rev. B*, Vol. 65, 195104, 2002.
17. Smith, D. R., D. C. Vier, T. Koschny, and C. M. Soukoulis, "Electromagnetic parameter retrieval from inhomogeneous metamaterials," *Phys. Rev. E*, Vol. 71, 036617, 2005.
18. Weir, W. B., "Automatic measurement of complex dielectric constant and permeability at microwave frequencies," *Proc. IEEE*, Vol. 62, 33–36, 1974.
19. Wirgin, A., "Optical properties of a noble metal with a string-of-pearls insulator inhomogeneity," *Physica A*, Vol. 157, 382–387, 1989.
20. Woodley, J. and M. Mojahedi, "On the signs of the imaginary parts of the effective permittivity and permeability in metamaterials," *J. Opt. Soc. Am. B*, Vol. 27, 1016–1021, 2010.